Inorg. Chem. **2002**, *41*, 3025–3031

Intramolecular Electronic Energy Transfer in Bichromophoric Macrocyclic Complexes

Paul V. Bernhardt,* Evan G. Moore, and Mark J. Riley

Department of Chemistry, University of Queensland, Brisbane, Australia, 4072

Received February 7, 2002

Efficient intramolecular electronic energy transfer (EET) has been demonstrated for three novel bichromophoric compounds utilizing a macrocyclic spacer as the bridge between the electronic energy donor and acceptor fragments. As their free base forms, emission from the electronically excited donor is absent and the acceptor emission is reductively quenched via photoinduced oxidation of proximate amine lone pairs. As their Zn(II) complexes, excitation of the donor results in sensitization of the electronic acceptor emission.

Introduction

The photophysical interactions between different chromophores of supramolecular systems have been a subject of appreciable interest.[1] The importance of electronic energy transfer during the photosynthetic process has spurred the design of potential biomimetic antennae involving porphyrins bearing covalently bound aromatic arenes such as naphthalene,[2] anthracene,[3] and pyrene.[4] Luminescent polypyridine−ruthenium(II) complexes bearing the same covalently bound arenes which show potential as light harvesting components have also been investigated.[5]

In general terms, the process of intramolecular electronic energy transfer (EET) in a bichromophoric molecule can be described by

$$\mathrm{D^*{-}B{-}A} \xrightarrow{k_{EET}} \mathrm{D{-}B{-}A^*}$$

where D* denotes an electronically excited donor moiety, A is a ground state acceptor, and B is a molecular bridge joining the two components. The first observation of short-range intramolecular EET in a bichromophoric naphthalene anthracene system was by Schnepp and Levy[6] where the bridge was a saturated alkyl chain of varying length [Nap−$(CH_2)_n$−Anth (n = 1, 2, 3)]. Compounds of this type still attract considerable current interest[7,8] and several molecules with more complex bridges are known which utilize the naphthalene and anthracene moieties as donor and acceptor fragments, respectively.[9] Considerably fewer examples of intramolecular EET utilizing combinations of naphthalene or anthracene with pyrene exist in the literature. Nonetheless, the ratio of donor and acceptor emission between these chromophores facilitated by EET has been used as a ruler to measure conformation changes in fluorescently labeled poly(ethyleneglycol) chains tethered to polystyrene.[10]

The experimental rate of energy transfer can often be simply attributed to two contributions, formulated by Förster[11] and Dexter.[12] The former is a long-range Coulombic interaction based on dipole−dipole interactions while the latter is a short-range interaction involving double electron exchange between overlapping donor and acceptor orbitals. As such, the efficiency of intramolecular energy transfer is critically dependent on the distance between the two chromophores.

In order to facilitate investigations of this distance dependence, bridges between components of increasing complexity have been developed.[13] Similarly, other effects

* Author to whom correspondence should be addressed. E-mail: bernhardt@chemistry.uq.edu.au.

(1) Speiser, S. *Chem. Rev.* **1996**, *96*, 1953.
(2) Fonda, H. N.; Gilbert, J. V.; Cormier, R. A.; Sprague, J. R.; Kamioka, K.; Connoly, J. S. *J. Phys. Chem.* **1993**, *97*, 7024.
(3) Cense, J. M.; Le Quax, R.-M. *Tetrahedron Lett.* **1979**, *39*, 3725.
(4) Treibs, A.; Haeberle, N. *Justus Liebigs Ann. Chem.* **1968**, *718*, 183.
(5) Wilson, G. J.; Launikonis, A.; Sasse, W. H. F.; Mau, W.-H. *J. Phys. Chem. A* **1997**, *101*, 4860.
(6) Schnepp, O.; Levy, M. *J. Am. Chem. Soc.* **1962**, *84*, 172.
(7) Rosenblum, G.; Grosswasser, D.; Schael, F.; Rubin, M.; Speiser, S. *Chem. Phys. Lett.* **1996**, *263*, 441.
(8) Wang, X.; Levy, D.; Rubin, M.; Speiser, S. *J. Phys. Chem. A* **2000**, *104*, 6558.
(9) Scholes, G.; Ghiggino, K.; Oliver, A.; Paddon-Row, N. *J. Phys. Chem.* **1993**, *97*, 11871.
(10) Jayachandran, K. N.; Maiti, S.; Chatterji, P. R. *Polymer* **2001**, *42*, 6113.
(11) Förster, T. *Discuss. Faraday Soc.* **1959**, *27*, 7.
(12) Dexter, D. *J. Chem. Phys.* **1953**, *21*, 836.
(13) Zimmerman, H.; Lapin, Y.; Nesterov, E.; Sereda, G. *J. Org. Chem.* **2000**, *65*, 7740.

10.1021/ic0255306 CCC: $22.00
Published on Web 04/30/2002

Chart 1

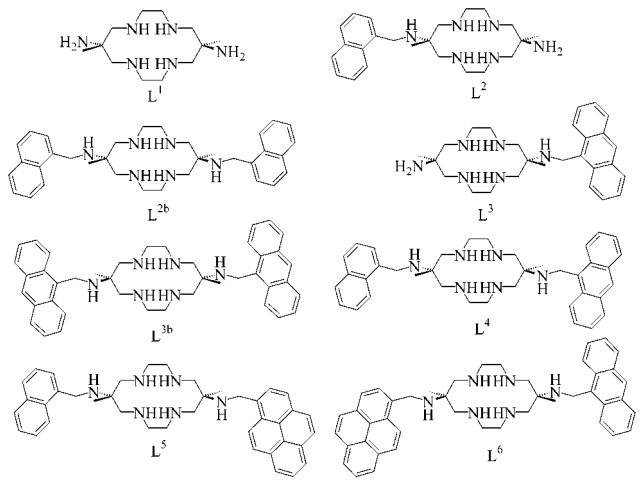

such as the relative orientation of the donor and acceptor chromophores which can significantly influence the rate of energy transfer via superexchange mechanisms have led to an increasing number of "rigid" rodlike organic bridges being developed such as bicyclo[1.1.1]pentane, bicyclo[2.2.2]-octane, adamantane, and cubane to name a few. The properties and syntheses of these and other novel bridges have been summarized in a recent review.[14]

With their increasing complexity, it was noted that solubility in polar solvents was a key problem in the synthesis of molecular rods and bridges. The attachment or incorporation of a charged group such as a transition metal ion to an otherwise poorly soluble molecular bridge would conceivably offer significantly increased solubility in polar solvents. Our experience with 13-, 14-, and 15-membered macrocyclic ligands bearing easily functionalized exocyclic pendant amino groups seemed an ideal place to unearth a potential new class of molecular bridges. We have previously shown[15] that complexation of these amine ligands with Zn(II) deactivates a ligand-based reductive quenching reaction mechanism, by analogy with other amino-substituted fluorophores, and the use of such bridges that can be "switched" may offer advantages in terms of selective signal transmission. To that end, we have utilized a 14-membered tetraaza macrocycle as a bridging unit between two aromatic chromophores, to yield the compounds displayed in Chart 1.

Experimental Section

Safety Note. All preparative work was carried out in the fume hood. Perchlorate salts are potentially explosive. Although no problems were encountered, they should be handled only in small quantities, never scraped from sintered glass frits nor heated in the solid state.

Syntheses. The parent macrocycle, *trans*-6,13-dimethyl-1,4,8,-11-tetraazacyclotetradecane-6,13-diamine hexahydrochloride, $L^1 \cdot 6HCl$, and anthracene-9-carbaldehyde were prepared according to previously reported methods.[16,17] Although the syntheses of the mono-substituted L^2 and L^3 ligands are known,[15,18] an improved method is outlined below using $NaBH_3CN$ in the reductive amination reaction, which gave much improved yields. Unless otherwise stated, all other reagents were obtained commercially and used as supplied without further purification.

***trans*-6,13-Dimethyl-*N*-naphthalen-1-ylmethyl-1,4,8,11-tetraazacyclotetradecane-6,13-diamine, L^2.** L^1 (0.52 g, 2.0 mmol) was dissolved in an $EtOH/H_2O$ mixture (9:1 v/v, 200 mL), and HCl (1 M) was added until the pH of the resulting clear solution was ca. 5.5. $Na[CN(BH_3)]$ (0.38 g, 6.0 mmol) was added, and the pH was readjusted to 5.5 with NaOH (1 M). Naphthalene-1-carbaldehyde (0.31 g, 2.0 mmol) was added, and the resulting solution was stirred at room temperature for ca. 2 h while the pH was maintained at ca. 5.5 by the addition of aliquots of HCl (1 M) as required. This solution was then stirred overnight, and a precipitate of *trans*-6,13-dimethyl-*N*,*N*′-bis-naphthalen-1-ylmethyl-1,4,8,11-tetraazacyclotetradecane-6,13-diamine (L^{2b}) as the biscyanoborohydride salt $[H_2L^{2b}][(CN)BH_3]_2$ was collected by vacuum filtration (0.13 g, 0.21 mmol, 10.5%). Excess EtOH was removed from the filtrate at reduced pressure, and H_2O (200 mL) was added. This solution was acidified to ca. pH 2 with HCl (1 M) and then extracted with CH_2Cl_2 (3 × 75 mL) to remove the reduced naphthalen-1-ylmethanol byproduct. The aqueous layer was kept, and the pH was adjusted to ca. 12 with NaOH (1 M). This was again extracted with CH_2Cl_2 (3 × 75 mL), and the organic layer was kept and dried over anhydrous Na_2SO_4. Removal of the solvent at reduced pressure gave the desired ligand, L^2, as an oil (0.60 g, 1.51 mmol, 75.3%). ^1H and ^{13}C NMR spectral data were identical to previously reported values.[15]

***N*-Anthracen-9-ylmethyl-*trans*-6,13-dimethyl-1,4,8,11-tetraazacyclotetradecane-6,13-diamine, L^3.** This ligand was prepared in a manner similar to that for L^2, but anthracene-9-carbaldehyde was substituted as the aromatic aldehyde. As with the previous synthesis, the homodisubstituted ligand *N*,*N*′-bis-anthracen-9-ylmethyl-*trans*-6,13-dimethyl-1,4,8,11-tetraazacyclotetradecane-6,13-diamine (L^{3b}) precipitated from the reaction solution as the biscyanoborohydride salt $[H_2L^{3b}][(CN)BH_3]_2$ (0.11 g, 5.1%). An identical workup of the filtrate as described gave the desired ligand, L^3, as an oil with an overall yield of ca. 58.1%. The ^1H and ^{13}C NMR spectra of this product were identical to those previously reported.[18]

***N*-Anthracen-9-ylmethyl-*trans*-6,13-dimethyl-*N*′-naphthalen-1-ylmethyl-1,4,8,11-tetraazacyclotetradecane-6,13-diamine, L^4.** The crude product L^2 (0.60 g, ca. 1.51 mmol) was redissolved in an $EtOH/H_2O$ mixture (9:1 v/v, 200 mL), and HCl (1 M) was added until the pH of the resulting clear solution was ca. 6.0. $Na[CN(BH_3)]$ (0.38 g, 6.0 mmol) was added, and the pH was readjusted to 6.0 with NaOH (1 M). Anthracene-9-carbaldehyde (0.31 g, 2.0 mmol) was dissolved separately in EtOH (50 mL) and then added, and the resulting solution was stirred at room temperature for ca. 2 h while the pH was maintained at ca. 6.0 by the addition of aliquots of HCl (1 M) as required. This solution was then stirred overnight to give a precipitate of the product as the biscyanoborohydride salt $[H_2L^4][(CN)BH_3]_2$, which was collected by vacuum filtration. This solid was suspended in H_2O (200 mL), and NaOH (3 M, 50 mL) was added. The resulting suspension was extracted with CH_2Cl_2 (3 × 75 mL) and dried over anhydrous Na_2SO_4, and removal of the solvent at reduced pressure gave the desired product as an oil. This was redissolved in CH_3CN, and the solvent was reduced in volume to give the ligand as a powdery solid (0.71 g, 70.3%).

(14) Schwab, P.; Levin, M.; Michl, J. *Chem. Rev.* **1999**, *99*, 1863.
(15) Bernhardt, P. V.; Moore, E. G.; Riley, M. J. *Inorg. Chem.* **2001**, *40*(23), 5799−5805.
(16) Bernhardt, P. V.; Lawrance, G. A.; Hambley, T. W. *J. Chem. Soc., Dalton Trans.* **1989**, 1059.
(17) Campaigne, E.; Archer, W. L. *J. Am. Chem. Soc.* **1953**, *75*, 989.
(18) Bernhardt, P. V.; Flanagan, B. M.; Riley, M. J. *J. Chem. Soc., Dalton Trans.* **1999**, 3579.

^{1}H NMR ($CDCl_3$): δ 1.23 (s, 3H, CH_3), 1.40 (s, 3H, CH_3), 1.9 (s br, 6H, NH), 2.5−2.8 (m, 16H, CH_2-macrocyclic), 4.17 (s, 2H, N−CH_2−Nap), 4.65 (s, 2H, N−CH_2−Anth), 7.3−7.5 (m, 8H), 7.75 (d, 1H), 7.84 (d, 1H), 7.98 (d, 2H), 8.25 (d, 1H), 8.37 (s, 1H), 8.43 (d, 2H).

^{13}C NMR ($CDCl_3$): δ 22.9, 23.0, 38.1, 43.9, 48.79, 48.84, 55.5, 55.9, 57.5, 57.7, 124.2, 124.5, 124.9, 125.5, 125.6, 125.84, 125.85, 126.4, 126.9, 127.6, 128.6, 129.0, 130.4, 131.6, 132.0, 132.2, 133.9, 136.9. Elemental anal. Found: C, 77.46; H, 8.34; N, 14.22. Calcd for $C_{38}H_{48}N_6$: C, 77.51; H, 8.22; N, 14.27.

***trans*-6,13-Dimethyl-*N*-naphthalen-1-ylmethyl-*N′*-pyren-1-ylmethyl-1,4,8,11-tetraazacyclotetradecane-6,13-diamine, L^5.** This ligand was prepared in a manner similar to that described for L^4, but pyrene-1-carbaldehyde was substituted as the aromatic aldehyde. As with the previous synthesis, the desired ligand precipitated from the reaction mixture as the biscyanoborohydride salt $[H_2L^5][(CN)BH_3]_2$. Using an identical workup of this solid yielded the desired ligand as the free base with typical yields of 70%.

^{1}H NMR ($CDCl_3$): δ 1.23 (s, 3H, CH_3), 1.30 (s, 3H, CH_3), 2.0 (s br, 6H, NH), 2.5−2.8 (m, 16H, CH_2-macrocyclic), 4.16 (s, 2H, N−CH_2−Nap), 4.41 (s, 2H, N−CH_2−Pyr), 7.4−7.5 (m, 4H), 7.75 (d, 1H), 7.84 (d, 1H), 7.9−8.2 (m, 8H), 8.25 (d, 1H), 8.49 (d, 1H).

^{13}C NMR ($CDCl_3$): δ 22.9, 23.1, 43.9, 44.2, 48.7, 55.5, 55.7, 57.61, 57.66, 123.7, 124.2, 124.8, 124.9, 125.0, 125.51, 125.56, 125.82, 125.87, 126.4, 127.0, 127.4, 127.5, 127.6, 128.6, 129.2, 130.6, 130.9, 131.3, 132.0, 133.8, 134.8, 136.8. Elemental anal. Found: C, 78.45; H, 8.04; N, 13.72. Calcd for $C_{40}H_{48}N_6$: C, 78.39; H, 7.89; N, 13.71.

***N*-Anthracen-9-ylmethyl-*trans*-6,13-dimethyl-*N′*-pyren-1-ylmethyl-1,4,8,11-tetraazacyclotetradecane-6,13-diamine, L.^{6}** The synthetic precursor for this ligand was the L^3 macrocycle, which was further functionalized by reaction with pyrene-1-carbaldehyde as described above. As with the previous two syntheses, the desired ligand precipitated from the reaction mixture as the biscyanoborohydride salt $[H_2L^6][(CN)BH_3]_2$. Identical workup of this solid yielded the desired ligand as the free base (yield ≅ 75%).

^{1}H NMR ($CDCl_3$): δ 1.29 (s, 3H, CH_3), 1.38 (s, 3H, CH_3), 2.0 (s br, 6H, NH), 2.6−2.9 (m, 16H, CH_2-macrocyclic), 4.39 (s, 2H, N−CH_2−Pyr), 4.61 (s, 2H, N−CH_2−Anth), 7.4−7.5 (m, 4H), 8.0−8.2 (m, 10H), 8.38 (s, 1H), 8.43 (d, 2H), 8.49 (d, 1H).

^{13}C NMR ($CDCl_3$): δ 22.9, 23.0, 38.1, 43.9, 48.79, 48.84, 55.5, 55.9, 57.5, 57.7, 124.2, 124.5, 124.9, 125.5, 125.6, 125.84, 125.85, 126.4, 126.9, 127.6, 128.6, 129.0, 130.4, 131.6, 132.0, 132.2, 133.9, 136.9. Elemental anal. Found: C, 79.84; H, 7.76; N, 12.81. Calcd for $C_{44}H_{50}N_6$: C, 79.72; H, 7.60; N, 12.68.

Physical Methods. Electronic absorption spectra were measured on a Perkin-Elmer Lambda 40 spectrophotometer using quartz cells. Emission spectra were collected on a Perkin-Elmer LS-50B spectrofluorimeter. Samples were purged with N_2 prior to measurements, and cutoff filters were employed to avoid higher order excitation light being detected. Nuclear magnetic resonance spectra were measured at 400.13 (^{1}H) and 100.62 MHz (^{13}C) on a Bruker AV400 spectrometer using $CDCl_3$ as solvent and tetramethylsilane (TMS) as reference.

Crystallography. Cell constants were determined by a least-squares fit to the setting parameters of 25 independent reflections measured on an Enraf-Nonius CAD4 four-circle diffractometer employing graphite-monochromated Mo Kα radiation (0.71073 Å) and operating in the $\omega-2\theta$ scan mode. Data reduction and empirical absorption corrections[19] (ψ-scans) were performed with the WINGX[20] package. Structures were solved by direct methods with SHELXS-86[21] and refined by full-matrix least-squares analysis against F^2 with SHELXL-97.[22] H atoms were included at estimated positions. Drawings of molecules were produced with PLATON97.[23]

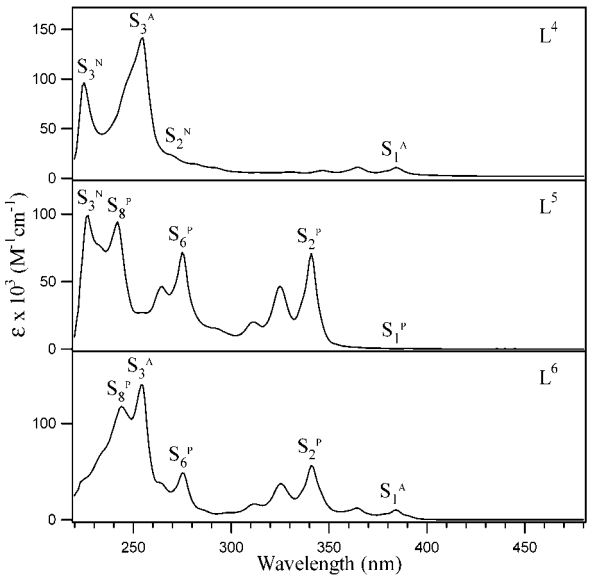

Figure 1. The electronic absorption spectra of the L^4, L^5, and L^6 ligands in MeOH.

Results

Electronic Absorption Spectroscopy. The electronic spectra of the three asymmetrically disubstituted bichromophoric ligands L^4, L^5, and L^6 were measured in MeOH and are shown in Figure 1. These spectra remain essentially unchanged upon coordination to Zn(II). The absorption spectrum of L^4 is dominated by both naphthalene and anthracene vibronic progressions. Two strong peaks apparent at 223 and 254 nm can be attributed to the naphthalene and anthracene $S_0 \rightarrow S_3$ transitions, respectively (labeled S_3^N and S_3^A in Figure 1).[24] These are slightly red shifted by comparison to the parent chromophores due to alkyl substitution.[25] At slightly lower energy, the naphthalene $S_0 \rightarrow S_2$ transition was evident as a shoulder at ca. 275 nm. The anthracene $S_0 \rightarrow S_2$ transition is only weakly electric dipole allowed and was not observed. Conversely, the $S_0 \rightarrow S_1$ absorption for this chromophore was clearly defined as a Franck−Condon vibrational progression with an origin at 385 nm and several peaks to higher energy separated by ca. 1420 cm^{-1}. The naphthalene $S_0 \rightarrow S_1$ transition is also only weakly electric dipole allowed and was not observed.

As with L^4, the electronic spectrum of L^5 showed the same strong naphthalene $S_0 \rightarrow S_3$ transition at 223 nm. By contrast, the highest energy absorption band of the pyrene chromophore observed was an intense peak at 241 nm, assigned previously[26] to the $S_0 \rightarrow S_8$ transition. A second band

(19) North A. C. T.; Phillips D. C.; Mathews F. S. *Acta Crystallogr., Sect. A* **1968**, *A24*, 351.
(20) Farrugia, L. J. *J. Appl. Crystallogr.* **1999**, *32*, 837.
(21) Sheldrick, G. M. *Acta Crystallogr., Sect. A* **1990**, *46*, 467.
(22) Sheldrick, G. M. *SHELXL-97: Program for Crystal Structure Refinement*; University of Göttingen: Göttingen, 1997.
(23) Spek, A. L. *Acta Crystallogr., Sect. A* **1990**, *46*, C34.
(24) Friedel, R. A.; Orchin, M. *Ultraviolet Spectra of Aromatic Compounds*; John Wiley & Sons: New York, 1951.
(25) Maiti, A. K. *Chem. Phys. Lett.* **1987**, *134*, 450.

appearing as a vibronic progression with an origin at 275 nm and peaks to higher energy separated by ca. 1515 cm^{-1} was similarly identified as the $S_0 \rightarrow S_6$ transition of the pyrene chromophore and completely concealed the $S_0 \rightarrow S_2$ transition of the naphthalene component. A vibrational progression originating from the pyrene chromophore $S_0 \rightarrow S_2$ absorption band was observed with an origin at 342 nm and two peaks to higher energy by ca.1435 cm^{-1} and ca.1275 cm^{-1}. The electronic transition to the lowest energy excited singlet state for the pyrene chromophore is only weakly electric dipole allowed, appearing at ca. 370 nm as denoted by S_1^P in Figure 1.

Absorption bands characteristic of the two aromatic components for the L^6 ligand were also evident with peaks at 241 and 254 nm for the pyrene $S_0 \rightarrow S_8$ and anthracene $S_0 \rightarrow S_3$ transitions, respectively. The pyrene $S_0 \rightarrow S_6$ transition again appeared at 275 nm while the $S_0 \rightarrow S_1$ transition for anthracene and $S_0 \rightarrow S_2$ transition for pyrene appeared as overlapping vibronic bands with their electronic origins at 385 and 342 nm, respectively. Higher energy vibrational peaks for the anthracene chromophore were observed at separations of ca.1420 cm^{-1} concealing the pyrene $S_0 \rightarrow S_1$ transition.

In summary, the absorption features of the bichromophoric ligands closely approximate the addition of the individual spectra for each component and thus it is reasonable to assume that excitation into bands identified with a particular chromophore will be largely localized on that moiety.

Emission and Excitation Spectroscopy. Emission spectra of the three ligands L^4, L^5, and L^6 were measured as their Zn(II) complexes in MeOH. These were prepared in situ by titration of 10^{-6} M solutions of the ligand with an equimolar amount of $Zn(OAc)_2 \cdot 2H_2O$.

For $[Zn(L^4)]^{2+}$, excitation directly into the intense anthracene $S_0 \rightarrow S_3$ transition at 254 nm gave a fluorescence spectrum as shown in Figure 2. Emission from the anthracene chromophore was evident as a Franck−Condon vibrational progression with an origin at 390 nm, a maximum intensity at 413 nm, and peak separations of ca. 1435 cm^{-1}. Identical results but with lower intensities were obtained when the $S_0 \rightarrow S_1$ transition was used as the excitation wavelength ($\lambda_{ex} = 365$ nm) since nonradiative relaxation to the lowest energy excited singlet state precedes fluorescence. Significantly, excitation of the naphthalene chromophore in the same complex at 223 or 275 nm also yields an emission spectrum identical to that obtained upon anthracene excitation.

The fluorescence excitation spectrum for $[Zn(L^4)]^{2+}$ obtained by monitoring anthracene emission at 413 nm (Figure 2) is almost identical to the electronic absorption spectrum of the complex, showing strong peaks from both aromatic chromophores. The peaks at 223 and 275 nm unmistakably originate from the naphthalene chromophore, and their appearance is indicative of electronic energy transfer from the higher to lower energy chromophore prior

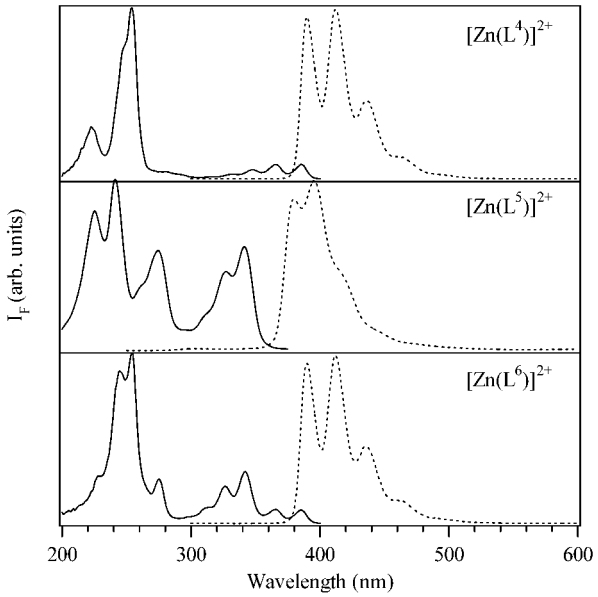

Figure 2. The fluorescence excitation (—) and emission (···) spectra for 10^{-5} M solutions of $[Zn(L^4)]^{2+}$, $[Zn(L^5)]^{2+}$, and $[Zn(L^6)]^{2+}$ in MeOH. Spectra are corrected for the wavelength dependence of the excitation lamp and detector response.

to anthracene fluorescence. The position and relative intensity of these excitation bands remain unchanged upon dilution (1:10), and the continued absence of naphthalene emission in the diluted sample reveals the energy transfer to be intra- rather than intermolecular.

Emission of the $[Zn(L^5)]^{2+}$ complex ($\lambda_{ex} = 241$ nm, see Figure 2) showed a maximum intensity at 395 nm with another peak to higher energy by ca.1275 cm^{-1}. This was assigned to emission from the lowest excited singlet state of the pyrene chromophore by comparison to analogous compounds.[10,27] Upon direct excitation of the naphthalene moiety at 223 nm, the only observable emission originates from the pyrene chromophore. The fluorescence excitation spectrum collected by monitoring this emission at 395 nm was measured and was similarly near identical to the electronic absorption spectrum of the complex, again indicative of electronic energy transfer from the naphthalene to pyrene chromophore. The $S_0 \rightarrow S_1$ transition of the pyrene chromophore absorbs only weakly, leading to a large Stokes shift between the excitation and emission bands, unlike the spectra of the $[Zn(L^4)]^{2+}$ complex where the 0−0 electronic origins are coincident.

The emission spectrum of $[Zn(L^6)]^{2+}$ was measured and is also shown in Figure 2. As with the $[Zn(L^4)]^{2+}$ complex, the spectrum contains emission bands which can be attributed solely to the lower energy anthracene chromophore independent of the excitation wavelength used with a maximum fluorescence intensity at ca. 413 nm. As with the previous two complexes, the fluorescence excitation spectra show peaks corresponding to absorption by both chromophores leading to emission by the anthracene component.

X-ray Crystallography. Crystals of either the free ligands or complexes of the asymmetrically disubstituted ligands L^{4-6}

(26) Salvi, P. R.; Foggi, P.; Castellucci, E. *Chem. Phys. Lett.* **1983**, *98*, 206.

(27) Bodenant, B.; Fages, F.; Delville, M.-H. *J. Am. Chem. Soc.* **1998**, *120*, 7511.

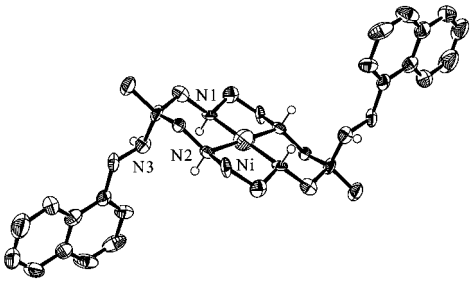

Figure 3. The crystal structure of the $[Ni(L^{2b})]^{2+}$ complex cation; 30% probability ellipsoids are shown. (Alkyl and aryl hydrogen atoms are omitted.)

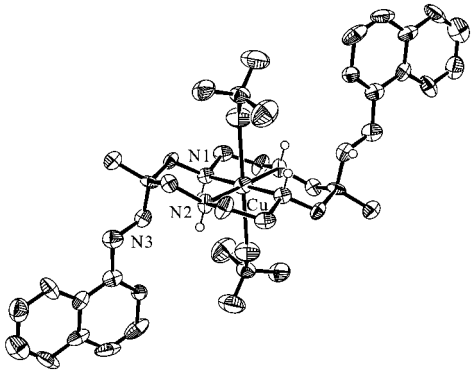

Figure 4. The crystal structure of the $[Cu(L^{2b})(ClO_4)_2]$ complex; 30% probability ellipsoids are shown. (Alkyl and aryl hydrogen atoms are omitted.)

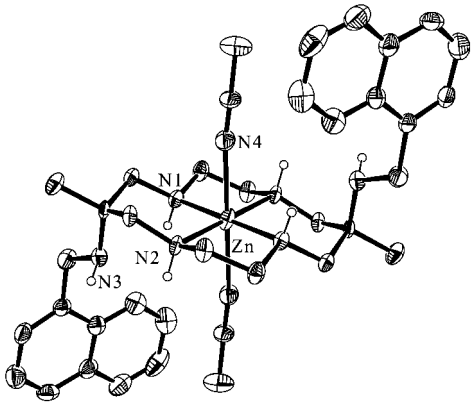

Figure 5. The crystal structure of the $[Zn(L^{2b})(CH_3CN)_2]^{2+}$ complex cation; 30% probability ellipsoids are shown. (Alkyl and aryl hydrogen atoms are omitted.)

have not been obtained. However, the symmetrically disubstituted Ni(II), Cu(II), and Zn(II) complexes of the L^{2b} ligand have been prepared and structurally characterized (Figures 3−5, Table 1). X-ray quality crystals were easily prepared by slow evaporation of an equimolar mixture of the ligand with the appropriate metal salt in the presence of excess $NaClO_4$ in CH_3CN.

The structure of $[Ni(L^{2b})](ClO_4)_2 \cdot (CH_3CN)_2$ is shown in Figure 3 and reveals a square planar complex with typical Ni−N bond lengths of ca. 1.95 Å. The nickel atom lies on a center of symmetry while perchlorate counteranions, although not coordinated, occupy general sites essentially above and below the macrocyclic plane in the axial position of the metal ion. Solvent acetonitrile molecules are found on general sites. The presence of two intramolecular hydrogen bonding interactions between the substituted secondary amino nitrogen and protons of the adjacent secondary amines is evident, with the shorter of the two interactions at 2.44 Å and the longer at 2.64 Å.

Table 1. Summary of Crystal Data

	$[Ni(L^{2b})](ClO_4)_2 \cdot (CH_3CN)_2$	$[Cu(L^{2b})(ClO_4)_2]$	$[Zn(L^{2b})(CH_3CN)_2](ClO_4)_2$
formula	$C_{38}H_{52}Cl_2NiN_8O_8$	$C_{34}H_{46}Cl_2CuN_6O_8$	$C_{38}H_{52}Cl_2ZnN_8O_8$
fw	878.49	795.16	886.52
cryst syst	monoclinic	triclinic	triclinic
space group	$P2_1/n$	$P\bar{1}$	$P\bar{1}$
a, Å	12.735(2)	8.412(1)	8.799(2)
b, Å	8.2791(7)	14.536(2)	9.929(1)
c, Å	20.136(2)	15.902(2)	12.403(2)
α, deg		104.76(1)	88.00(1)
β, deg	104.81(1)	98.98(1)	85.76(1)
γ, deg		106.44(1)	74.82(1)
V, Å^3	2052.5(4)	1748.0(4)	1042.8(3)
Z	2	2	1
T, K	293(2)	293(2)	293(2)
λ, Å	0.71073	0.71073	0.71073
μ, cm^{-1}	6.64	8.39	13.26
ρ_{calcd}	1.421	1.511	1.412
$R(F_o)^a$	0.1078	0.0723	0.0762
wR2(F_o)^b	0.2782	0.3420	0.2870

^{a} $R(F_o) = \sum||F_o| - |F_c||/\sum|F_o|$. ^{b} $wR2(F_o^2) = (\sum w(F_o^2 - F_c^2)/\sum wF_o^2)^{1/2}$.

Table 2. Selected Bond Lengths (Å) and Angles (deg)

	$[Ni(L^{2b})](ClO_4)_2 \cdot (CH_3CN)_2$	$[Cu(L^{2b})(ClO_4)_2]$	$[Zn(L^{2b})(CH_3CN)_2](ClO_4)_2$
M−N1	1.930(8)	2.025(8)	2.076(7)
M−N2	1.960(9)	1.974(9)	2.052(7)
M−N4/O1		2.54(1)	2.341(9)
Nap−Nap	14.98	15.02	12.73
N1−M−N2	90.5(4)	93.8(4)	93.6(3)

The $[Cu(L^{2b})(ClO_4)_2]$ complex is shown in Figure 4 and reveals a tetragonally distorted octahedral coordination geometry about the metal ion. The triclinic unit cell contains two independent centrosymmetric complex cations. As with the known structures[28−30] of [Cu(cyclam)$(ClO_4)_2$] and [Cu$(L^1)(ClO_4)_2$], perchlorate counteranions are bound axially perpendicular to the macrocyclic plane. The observed Cu−O and Cu−N bond lengths (Table 2) are typical for complexes of this type. Both cations also display intramolecular hydrogen bonding interactions between the exocyclic substituted amino nitrogen lone pair and protons of the macrocyclic nitrogen donors.

The $[Zn(L^{2b})(CH_3CN)_2](ClO_4)_2$ complex is shown in Figure 5, and the coordination geometry about the metal ion can again be described as a tetragonally distorted octahedron. Four macrocyclic nitrogen donors are bound equatorially to the Zn(II) with typical Zn−N bond lengths of ca. 2.05 Å while coordinated solvent acetonitrile molecules complete the first coordination sphere. The metal ion is again on a center of symmetry while unbound perchlorate counteranions on general sites complete the remainder of the asymmetric unit. Again, as with the Ni(II) and Cu(II) structures, the same intramolecular hydrogen bonding pattern is apparent in the

(28) Tasker, P. A.; Sklar, L. *J. Cryst. Mol. Struct.* **1975**, *5*, 329.
(29) Lawrance, G. A.; Skelton, B. W.; White, A. H.; Comba, P. *Aust. J. Chem.* **1986**, *39*, 1101.
(30) Bernhardt, P. V.; Jones, L. A.; Sharpe, P. C. *J. Chem. Soc., Dalton Trans.* **1997**, 1169.

Zn(II) complex with distances of 2.46 and 2.53 Å for N3···H1−(N1) and N3···H2−(N2), respectively.

In all three structures, the ligand has adopted the common *trans*-III configuration of nitrogen donors first noted in cyclam due to the inherent stability associated with the alternating gauche and chair conformations of five- and six-membered chelate rings, respectively.[31] The pendant amine groups similarly all have an axial (α) disposition with respect to the six-membered chelate rings to which they are bound. This configuration has been found in all structurally characterized derivatives of L^1 where one or both pendant amines have undergone alkylation.

Discussion

Electronic spectra of the three bichromophoric ligands studied both as the free ligands and the Zn(II) complexes were found to be simple superpositions of the spectra of the individual components. Absorption peaks were in good agreement with the parent aromatic chromophores, and the absence of any new bands is indicative of negligible ground state interaction between the two π electron systems of the components.

Upon excitation, the emission spectra for each of the Zn(II) complexes displayed peaks which were characteristic of the chromophore with the lowest energy first excited singlet state, even when excitation was to a state localized on the donor chromophore. The fluorescence excitation spectra monitored at the peak emission wavelengths also revealed absorption by both the donor and acceptor constituents leading to emission solely by the acceptor. The absence of donor emission, which persisted upon serial dilution of the samples, is indicative of an intramolecular EET process. Furthermore, the ratio of donor and acceptor absorption in the fluorescence excitation spectra was constant for solutions of differing concentration. If the EET were intermolecular, a change in the relative acceptor emission after excitation into a donor absorption band compared to direct excitation via the acceptor would be expected. These results attest to highly efficient intramolecular energy transfer occurring in the Zn(II) complexes of all three ligands.

From the steady state measurements presented, the exact mechanism for the energy transfer process cannot be fully elucidated. The interchromophore separations obtained from the Ni(II), Cu(II), and Zn(II) solid state structures of the L^{2b} ligand ranged from ca. 12 to 15 Å (Table 2), and it is likely that this range would be essentially the same for the asymmetrically disubstituted L^4, L^5, and L^6 ligands. This separation combined with the trans disposition of the pendant amino attachment points with respect to the macrocyclic plane would appear to prohibit any direct orbital interactions between the two chromophores thus eliminating energy transfer by the Dexter mechanism as a possibility.

Since the relevant transitions are electric dipole allowed with intense oscillator strengths, the Coulombic mechanism for dipole−dipole mediated energy transfer proposed by Förster is facilitated in these bichromophoric compounds. The possibility of EET occurring via a long-range exchange mechanism ("superexchange") involving through-bond coupling cannot be discarded, however, as it has been found that rigid hydrocarbon bridges can effect considerable orbital overlapping between distant donor and acceptor moieties.[9] In our systems, the macrocycle can be considered rigid; however, free rotation of the appended aromatic chromophores may well imbue sufficient flexibility to suppress these interactions.

For the purpose of evaluating the mechanism of short-range intramolecular EET, the macrocyclic bridge presented here satisfies a number of essential criteria and offers a number of potential advantages. We have shown that it acts simply as an inert molecular spacer and does not influence the basic electronic structure of the appended chromophores. Similarly, as evidenced from the crystal structures of L^{2b} with Ni(II), Cu(II), and Zn(II), the macrocycle adopts a well-defined *trans*-III configuration of nitrogen donors and the pendant amine groups all have axial (α) dispositions with respect to their six-membered chelate rings. As such, the distance between the pendant amine attachment points is essentially invariant.

As anticipated, the introduction of a metal ion within the macrocyclic bridge was also very effective in conveying solubility in polar solvents in which the free ligand was otherwise only moderately soluble. Indeed, the presence of Zn(II) not only enhances solubility but is essential for electronic energy transfer; otherwise photoinduced electron transfer (PET) from amine lone pairs leads to significant reductive quenching of the acceptor emission. In a previous paper,[15] it was suggested that the substituted pendant amines of the L^2 macrocycle were most likely coordinated to the metal ion, as is the case for $[Zn(L^1)]^{2+}$, and hence could not undergo photoinduced oxidation. The crystal structure reported here for $[Zn(L^{2b})(CH_3CN)_2](ClO_4)_2$ shows that this is not the case, at least for the symmetrically disubstituted compound in the solid state. It is likely that the L^4, L^5, and L^6 ligands will display coordination environments similar to that of L^{2b}. Presumably, the significant decrease in PET fluorescence quenching is due to the presence of strong intramolecular hydrogen bonds between the free amine lone pair and protons of the adjacent secondary amino groups, thus raising the ionization potential at the free amine. In addition, the close proximity of a dipositive metal ion may inhibit PET reactivity by an inductive effect.

Conclusions

Several new bichromophoric compounds have been prepared and characterized as the "free" ligands and as the corresponding Zn(II) complexes. Efficient intramolecular electronic energy transfer has been demonstrated in each of the complexes over distances of ca. 12−15 Å, which can be attributed to the Förster mechanism for long-range Coulombic interactions. The macrocyclic bridging unit represents a

(31) Bosnich, B.; Poon, C. K.; Tobe, M. L. *Inorg. Chem.* **1965**, *4*, 1102.

different class of linker between donor and acceptor moieties with a predetermined "semirigid" geometry enforced by coordination to a central metal ion, offering enhanced solubility in polar solvents as an additional benefit. The weakly fluorescent free ligands have their emission activated upon coordination to Zn(II). These switchable electronic energy transfer systems may have potential applications in the developing field of molecular electronics and optics.

Acknowledgment. Financial support by the Australian Research Council and the Australian Institute for Nuclear Science and Engineering is gratefully acknowledged.

Supporting Information Available: Crystallographic data in CIF format. This material is available free of charge via the Internet at http://pubs.acs.org.

IC0255306